

# A BDDC ALGORITHM WITH DELUXE SCALING FOR THREE-DIMENSIONAL $H(\text{CURL})$ PROBLEMS

CLARK R. DOHRMANN\* AND OLOF B. WIDLUND†

TR2014-964

**Abstract.** In this paper, we present and analyze a BDDC algorithm for a class of elliptic problems in the three-dimensional  $H(\text{curl})$  space. Compared with existing results, our condition number estimate requires fewer assumptions and also involves two fewer powers of  $\log(H/h)$ , making it consistent with optimal estimates for other elliptic problems. Here,  $H/h$  is the maximum of  $H_i/h_i$  over all subdomains, where  $H_i$  and  $h_i$  are the diameter and the smallest element diameter for the subdomain  $\Omega_i$ . The analysis makes use of two recent developments. The first is a new approach to averaging across the subdomain interfaces, while the second is a new technical tool which allows arguments involving trace classes to be avoided. Numerical examples are presented to confirm the theory and demonstrate the importance of the new averaging approach in certain cases.

**1. Introduction.** The design and analysis of domain decomposition algorithms for problems formulated in the three-dimensional  $H(\text{curl})$  space pose quite significant challenges, a fact reflected in a small number of archival publications. Pioneering work was done by Qiya Hu and Jun Zou [11, 12], who developed a wire basket algorithm for a positive definite, self-adjoint problem and for a saddle-point problem. Their work has been resumed more recently and has resulted in two papers, [9, 10], coauthored with Shi Shu. Other major contributions are by Andrea Toselli [22], an important study of FETI–DP algorithms, and by Toselli [21] and Ralf Hiptmair and Toselli [6] on two-level overlapping Schwarz algorithms.

This paper concerns a BDDC algorithm for problems with the same positive definite, self-adjoint bilinear form considered in Toselli [22]:

$$a(\mathbf{v}, \mathbf{w}) := \sum_i (\alpha_i (\nabla \times \mathbf{v}_i, \nabla \times \mathbf{w}_i)_{L^2(\Omega_i)} + \beta_i (\mathbf{v}_i, \mathbf{w}_i)_{L^2(\Omega_i)}), \quad (1.1)$$

where  $\mathbf{v}_i$  and  $\mathbf{w}_i$  are restrictions, to  $\Omega_i$ , of elements of  $H_0(\text{curl}, \Omega)$ , the subspace of  $H(\text{curl}, \Omega)$  with a zero tangential trace on  $\partial\Omega$ . The  $\alpha_i \geq 0$  and the  $\beta_i > 0$  are constants and the  $\Omega_i$  are subdomains into which the domain  $\Omega$  of the given problem has been partitioned. We note that the inner product of the space  $H(\text{curl}, \Omega)$ , for a domain of diameter 1, is given by (1.1) after setting all  $\alpha_i$  and  $\beta_i$  equal to 1. Not to complicate things further, we will assume that the  $\Omega_i$  are all homotopy equivalent to a ball.

While some of our technical tools differ considerably from Toselli’s, we have been able to draw significantly on his insights. Given that FETI–DP and BDDC algorithms are closely related, see [18, 2, 17], our results also improve those of Toselli. We note that we have previously published a conference paper [4] on a different and computationally less attractive BDDC algorithm, which essentially is Toselli’s Algorithm C. Our BDDC deluxe algorithm was first introduced in that paper and has already been used, with considerable success, for several different problem classes, see [3, 16, 20].

---

\*Computational Solid Mechanics and Structural Dynamics Department, Sandia National Laboratories, Albuquerque, New Mexico, 87185 [crdohrm@sandia.gov](mailto:crdohrm@sandia.gov). Sandia is a multiprogram laboratory operated by Sandia Corporation, a Lockheed Martin Company, for the United States Department of Energy’s National Nuclear Security Administration under Contract DE-AC04-94-AL85000.

†Courant Institute, 251 Mercer Street, New York NY 10012, USA [widlund@cims.nyu.edu](mailto:widlund@cims.nyu.edu), <http://www.cs.nyu.edu/cs/faculty/widlund>. This work was supported in part by the U.S. Department of Energy under contracts DE-FG02-06ER25718 and in part by the National Science Foundation Grant DMS-1216564.

In summary, we have two fewer powers of  $\log(H/h)$  in our condition number estimate than Toselli making our results the best possible. Moreover, the assumptions on the material parameters are relaxed as well. In our technical work, we follow the example of Dryja, Smith, and one of the authors, see [5] and [23, Chapter 4], and develop bounds for minimal energy extensions of functions defined on subdomain boundaries by explicitly constructing extensions with comparable energy. In this way, arguments involving trace classes can be avoided. We note that trace theorems for  $H(\text{curl})$  are more complicated than those for  $H^1$ ; cf., e.g., the discussion in [22]. We also hope that our strategy will make our paper more accessible.

Given that we aim at developing bounds that are independent of the values of the material coefficients, we also strive at finding arguments that can be reduced to work on individual subdomains. This has been accomplished except, like Toselli's, our bound contains a factor  $\eta := (1 + \max_i \beta_i H_i^2 / \alpha_i)$ , where  $H_i$  denotes the diameter of the subdomain  $\Omega_i$ . Thus, if we have any mass-dominated subdomains for which  $\beta_i H_i^2 / \alpha_i$  is large, our bound and the performance of the algorithm will be less satisfactory. Subdomains that are not mass-dominated are said to be curl-dominated.

The rest of the paper is organized as follows. In Section 2, we introduce our problem and review the Nédélec finite element space. We also introduce our deluxe version of the BDDC domain decomposition algorithm. In Section 3, we collect some technical tools that are well known from the study of elliptic problems posed in  $H^1(\Omega)$ . We also formulate and prove new bounds for  $H(\text{curl}, \Omega)$  and cite a result by Hiptmair and Xu [8] that is important for our development of the theory, which is given in Section 4. We note that their algorithm has formed the basis of important software and that has been extensively tested; see Kolev and Vassilevski [15]. Implementation details, for our algorithm, in particular for problems with irregular subdomains obtained from mesh partitioners, are discussed in Section 5. Finally, results of numerical experiments are given in Section 6.

**2. Our Problem and Our Algorithm.** We will focus on developing and analyzing a domain decomposition method for problems discretized by the lowest order Nédélec elements, introduced in [19], with unknowns given for the edges of the tetrahedral elements into which the given domain  $\Omega$  has been partitioned. We will also introduce our BDDC variant in this section.

**2.1. The Finite Element Space.** The space of Nédélec finite element functions can be represented as the range of an interpolation operator  $\Pi^h$  which is well defined, for sufficiently smooth elements of  $\mathbf{w} \in H(\text{curl}, \Omega)$ , by

$$\Pi^h(\mathbf{w}) := \sum_e \lambda_e(\mathbf{w}) \mathbf{N}_e \quad \text{where} \quad \lambda_e(\mathbf{w}) := \frac{1}{|e|} \int_e \mathbf{w} \cdot \mathbf{t}_e ds.$$

Here  $\mathbf{t}_e$  is a unit vector in the direction of the element edge  $e$ . The restriction of the basis function  $\mathbf{N}_e(\mathbf{x})$  to an element  $K$  is of the form  $\mathbf{N}_e(\mathbf{x}) := \mathbf{a}_e^K + \mathbf{b}_e^K \times \mathbf{x}$  where the six real parameters of  $\mathbf{a}_e^K$  and  $\mathbf{b}_e^K$  of each element are determined so that  $\lambda_e(\mathbf{N}_e) = 1$  while  $\lambda_{e'}(\mathbf{N}_e) = 0$  for any other edge  $e'$  of the triangulation. For the element edges along a subdomain edge  $E$ , we will always assume that the unit vectors  $\mathbf{t}_e$  all point in the same direction as a unit vector  $\mathbf{t}_E$  of the subdomain edge  $E$ . In subsection 4.2, we also need to make sure that the unit vectors  $\mathbf{t}_E$  do not change direction when we move from one subdomain edge to the next following the boundary of a subdomain face.

The interface between the subdomains is  $\Gamma := \cup_{i=1}^N \partial\Omega_i \setminus \partial\Omega$ . Similarly,  $\Gamma_i := \partial\Omega_i \setminus \partial\Omega$ . We will always assume that the  $\Gamma_i$  do not cut through any elements and,

when developing the theory, that the  $\Omega_i$  are polyhedra with planar faces. A subdomain face  $F$  is the interior of the intersection of two subdomain boundaries  $\partial\Omega_i$  and  $\partial\Omega_j$ ; it thus is a face of the polyhedron  $\Omega_i$  or the union of several such faces and the subdomain edges between them. We note that a subdomain face need not necessarily be planar. In our technical work, we will assume that our subdomain faces satisfy the following assumption:

ASSUMPTION 1. *Each subdomain face satisfies one of the following conditions:*

- *It is a star-shaped polygon, i.e., a polygon in the plane which is a star domain. There then exists a point  $c_F \in F$  such that the line segment between  $c_F$  and any other point of  $F$  belongs to  $F$ .*
- *There is a unique subdomain vertex  $c_F$  in the interior of  $F$ .*

*In all cases, we further assume that the triangles created by connecting the point  $c_F$  and the vertices of the boundary  $\partial F$  are shape regular.*

More general subdomain faces could also be considered but we have chosen to confine our proofs to those satisfying this assumption in the interest of simplicity.

We will denote by  $\mathcal{M}_{\Gamma_i}$ ,  $\mathcal{M}_F$ , and  $\mathcal{M}_{\partial F}$  the sets of finite element edges on  $\Gamma_i$ ,  $F$ , and  $\partial F$ , respectively. The set  $\mathcal{M}_{F_b}$  contains all element edges on  $F$  which have an endpoint on  $\partial F$ . We also denote by  $\mathcal{N}_E$  and  $\mathcal{N}_{\partial F}$ , the set of nodes on  $E$  and  $\partial F$ , respectively.

We will denote by  $W_{\text{curl}}^{h_i}$  the space of lowest order Nédélec elements, just introduced, and by  $W_{\text{grad}}^{h_i}$  the space of continuous, piecewise linear finite element functions on the subdomain  $\Omega_i$  for the same triangulation. We note that the gradient operator  $\nabla$  maps  $W_{\text{grad}}^{h_i}$  into a subspace of  $W_{\text{curl}}^{h_i}$  and that it is also well known that any element of the form  $\Pi^h \nabla p$ ,  $p \in H^1(\Omega_i)$ , is curl-free and that there are positive constants  $c$  and  $C$ , which depend only on the shape-regularity of the elements, such that

$$c \sum_{e \in \partial K} h_i^3 |\lambda_e(\mathbf{w}_h)|^2 \leq \|\mathbf{w}_h\|_{L^2(K)}^2 \leq C \sum_{e \in \partial K} h_i^3 |\lambda_e(\mathbf{w}_h)|^2, \quad \forall \mathbf{w}_h \in W_{\text{curl}}^{h_i} \quad (2.1)$$

$$\|\nabla \times \mathbf{w}_h\|_{L^2(K)}^2 \leq C \sum_{e \in \partial K} h_i |\lambda_e(\mathbf{w}_h)|^2, \quad \forall \mathbf{w}_h \in W_{\text{curl}}^{h_i}, \quad (2.2)$$

and

$$\|\nabla \times \Pi^h(\mathbf{u}_h)\|_{L^2(K)} \leq C \|\mathbf{u}_h\|_{H^1(K)}, \quad \forall \mathbf{u}_h \in W_{\text{grad}}^{h_i}. \quad (2.3)$$

These bounds can be derived easily by working on an individual element  $K$  and by using an elementary inverse inequality.

Certain index sets are important when developing and implementing iterative substructuring algorithms. We divide the element edges on  $\Gamma_i$  into equivalence classes determined by the sets of  $\Gamma_j$  to which they belong. Thus, for the case at hand, we have an equivalence class for each subdomain edge and one for each subdomain face; that for a subdomain face has two indices and that for a subdomain edge typically has three or more. We note that for irregular subdomains such as those obtained by mesh partitioners, there can be good reasons to divide some of the equivalence classes; see further Section 5.

The success of any iterative substructuring algorithm depends significantly on the existence of a stable decomposition of any finite element function, defined by its values on  $\Gamma$ , into a sum of functions each associated exclusively with the degrees of freedom of one equivalence class. As is convincingly argued by Toselli [22], there is a strong

coupling between subdomain faces and subdomain edges, which precludes a good decomposition and fast algorithms, if the original basis of the Nédélec space is used. We will therefore use an alternative basis, as in [22]. Thus, for each subdomain edge  $E$ , we will use two functions  $\Phi_E$  and  $\nabla\phi_{iE}$ , the *constant* and the *gradient* components associated with the subdomain edge  $E$ . Here,  $\Phi_E \cdot \mathbf{t}_e = 1$  for all element edges  $e \subset E$  while it vanishes on all other element edges on  $\Gamma$  and  $\phi_{iE}$  is a linear combination of the standard basis functions of  $W_{\text{grad}}^{h_i}$  for the nodes in the interior of the edge  $E$ . We then find that

$$\mathbf{w}_i \cdot \mathbf{t}_e = a_E(\mathbf{w}_i)\Phi_E \cdot \mathbf{t}_e + \nabla\phi_{iE} \cdot \mathbf{t}_e = a_E(\mathbf{w}_i) + \nabla\phi_{iE} \cdot \mathbf{t}_e, \quad \forall e \in E, \quad (2.4)$$

where  $a_E(\mathbf{w}_i)$  is the average of  $\mathbf{w}_i \cdot \mathbf{t}_e$  over  $E$ .

REMARK 1. *While we will fully develop our theory only for polyhedral subdomains, for which the subdomain edges are straight, we have also developed our algorithm for a more general case. Thus, for an edge  $E$  that is not straight, we define the function  $\Phi_E$  by the alternative formula  $\Phi_E \cdot \mathbf{t}_e := \mathbf{d}_E \cdot \mathbf{t}_e$ , where  $\mathbf{d}_E$  is a unit vector pointing in direction from one endpoint of  $E$  to the other. We note that the integral of the gradient component associated with the edge  $E$ , over the edge, will always vanish.*

**2.2. BDDC deluxe.** We will primarily consider a recently introduced variant of BDDC known as BDDC deluxe. The BDDC and FETI-DP algorithms are iterative substructuring algorithms, i.e., they are based on non-overlapping decompositions  $\{\Omega_i\}_{i=1}^N$  of the domain  $\Omega$  on which the problem is posed.

Any BDDC or FETI-DP algorithm is determined by a set of primal constraints and by an average or a jump operator, respectively. We will focus exclusively on a primal constraint set given by two moments for each subdomain edge. Thus,

$$s_{0E}(\mathbf{w}_i) := (1/|E|) \int_E \mathbf{w}_i \cdot \mathbf{t}_e \, ds, \quad (2.5)$$

$$s_{1E}(\mathbf{w}_i) := (1/|E|) \int_E s\mathbf{w}_i \cdot \mathbf{t}_e \, ds, \quad (2.6)$$

will take on the same values for any two subdomains which share a subdomain edge  $E$ . Here  $s \in [-|E|/2, |E|/2]$  is an arc length parameter. This choice of constraints is also used for Toselli's Algorithm B. Toselli also demonstrated that using only the first constraint, defined by (2.5), results in a considerably much slower algorithm. We note that  $s_{0E}(\Phi_E) = 1$  and that  $s_{0E}(\nabla\phi_{iE}) = 0$ , since  $\phi_{iE}$  vanishes at the endpoints of the edge. Given that  $s_{0E}(\mathbf{w}_i) = s_{0E}(\mathbf{w}_k)$  for two subdomains  $\Omega_i$  and  $\Omega_k$  sharing  $E$ , it then follows that  $a_E(\mathbf{w}_i) = a_E(\mathbf{w}_k)$ . Again by using that the nodal function  $\phi_{iE}$  vanishes at the endpoints of  $E$ , we see, by using (2.4) and by integrating by parts, that

$$s_{1E}(\nabla\phi_{iE}) = -\bar{\phi}_{iE} \quad (2.7)$$

where  $\bar{\phi}_{iE}$  is the average of  $\phi_{iE}$  over  $E$ . Thus, since  $s_{1E}(\Phi_E) = 0$  and  $s_{1E}(\mathbf{w}_i) = s_{1E}(\mathbf{w}_k)$ , it follows that  $\bar{\phi}_{iE} = \bar{\phi}_{kE}$ .

In order to simplify the description of the algorithm, we will make a further change of variables, as in [17]. This change of basis is confined to the variables associated with the subdomain edges. In addition to the degree of freedom associated with the average  $a_E(\mathbf{w}_i)$ , we introduce a variable given in terms of (2.6), the other moment over the subdomain edge, and a complementary set of variables, with basis functions for which

the two moments vanish. We next group the two special variables for each subdomain edge, for which the primal constraints are enforced, into the *primal* subspace while the subspace of the remaining degrees of freedom of  $\Gamma_i$  is called the *dual* subspace.

We will work with three spaces,  $W_\Gamma$ , the direct sum of the spaces of subdomain traces  $W_{\Gamma_i}^{(i)}$  of the Nédélec functions, without any continuity across the interface, the partially assembled space  $\widetilde{W}_\Gamma$ , i.e., the product space with common values of the primal variables, and  $\widehat{W}_\Gamma$  with common values of all tangential components across the interface.

Let us now consider the stiffness matrix associated with the subdomain  $\Omega_i$  :

$$A^{(i)} := \begin{pmatrix} A_{II}^{(i)} & A_{I\Delta}^{(i)} & A_{I\Pi}^{(i)} \\ A_{\Delta I}^{(i)} & A_{\Delta\Delta}^{(i)} & A_{\Delta\Pi}^{(i)} \\ A_{\Pi I}^{(i)} & A_{\Pi\Delta}^{(i)} & A_{\Pi\Pi}^{(i)} \end{pmatrix}.$$

Here  $I$  represents the degrees of freedom of the element edges in the interior of  $\Omega_i$ , i.e., those of the set  $\mathcal{M}_{\Omega_i}$ ,  $\Delta$  those of the dual variables on  $\Gamma_i$ , and  $\Pi$  those of the primal variables. After eliminating the interior degrees of freedom, by Gaussian elimination, we obtain the subdomain Schur complement

$$S^{(i)} := \begin{pmatrix} S_{\Delta\Delta}^{(i)} & S_{\Delta\Pi}^{(i)} \\ S_{\Pi\Delta}^{(i)} & S_{\Pi\Pi}^{(i)} \end{pmatrix} := \begin{pmatrix} A_{\Delta\Delta}^{(i)} & A_{\Delta\Pi}^{(i)} \\ A_{\Pi\Delta}^{(i)} & A_{\Pi\Pi}^{(i)} \end{pmatrix} - \begin{pmatrix} A_{\Delta I}^{(i)} \\ A_{\Pi I}^{(i)} \end{pmatrix} \left( A_{II}^{(i)} \right)^{-1} \begin{pmatrix} A_{I\Delta}^{(i)} & A_{I\Pi}^{(i)} \end{pmatrix}.$$

We have thus partitioned  $\mathbf{w}_{i\Gamma}$  into two subvectors, the dual  $\mathbf{w}_{i\Delta}$  and the primal  $\mathbf{w}_{i\Pi}$ . We note that we do not need to compute the elements of  $S^{(i)}$  explicitly, since we can instead use the formula for the Schur complement, to compute the product of  $S^{(i)}$  times a vector and that we similarly can compute the action of its inverse on a vector by solving a linear system with the matrix  $A^{(i)}$ . The right hand side  $\mathbf{f}^{(i)}$  of such a system then should satisfy  $\mathbf{f}_I^{(i)} = 0$ .

The stiffness matrix of the original linear system of equations,  $\widehat{A}$ , is obtained by subassembling the subdomain stiffness matrices  $A^{(i)}$ . By locally eliminating the interior variables of all the subdomains, we obtain a reduced linear system with all components, interior to the subdomains, no longer present, and with a matrix  $\widehat{S}_\Gamma$  which can also be obtained by subassembling the subdomain Schur complements  $S^{(i)}$ .

When building our preconditioner, we will also use a partially subassembled Schur complement  $\widetilde{S}_\Gamma$  defined on the intermediate space  $\widetilde{W}_\Gamma$ . We note that when solving a linear system with that matrix, we can take advantage of the fact that the dual variables effectively are local variables allowing them to take on multiple values; the number of variables that couple the subdomain problems together globally is thus much smaller than for a fully assembled model. We also note that when we need to solve a linear system with the matrix  $\widetilde{S}_\Gamma$ , we can equally well solve a linear system of equations with the matrix  $\widehat{A}$  obtained by partially subassembling the matrices  $A^{(i)}$ , again allowing the dual variables on  $\Gamma$  to take on multiple values.

At the end of each BDDC iteration step, the approximate solution is made continuous across the interface with continuity restored by applying a weighted average operator  $E_D$ , which maps  $\widetilde{W}_\Gamma$  into  $\widehat{W}_\Gamma$ .

A step of our BDDC algorithm is as follows: In each iteration, we first compute the residual of the fully assembled Schur complement equation. We then apply  $E_D^T$  to obtain the right-hand side of the partially subassembled Schur complement system of equations with the matrix  $\widetilde{S}_\Gamma$ . We then solve this system and apply  $E_D$  to the solution.

Averaging will change the values on  $\Gamma$ , and unless the iteration already has converged, and if the averaging only involves values on  $\Gamma$ , this gives rise to non-zero residuals at nodes next to those on  $\Gamma$ . Finally, these new residuals are eliminated by solving Dirichlet problems on each of the subdomains. This last step will not be required for the new variant of the BDDC algorithm since no such residuals will appear. We accelerate the iteration by using the preconditioned conjugate gradient method.

The average  $\bar{\mathbf{w}} := E_D \mathbf{w}$  of an element in  $\mathbf{w} \in \bar{W}$ , is computed separately for the interface degrees of freedom of the different equivalence classes. We recall that each of these classes is defined by the index set of the subdomain interfaces  $\Gamma_j$  to which the interface degrees of freedom belong. For a class with only two elements,  $i$  and  $j$ , associated with a subdomain face  $F$ , we define minors of two subdomain Schur complements by  $S_F^{(i)} := R_F^{(i)} S^{(i)} R_F^{(i)T}$  and  $S_F^{(j)} := R_F^{(j)} S^{(j)} R_F^{(j)T}$ , where  $R_F^{(i)}$  is the restriction operator from  $\mathcal{M}_{\Gamma_i}$  to  $\mathcal{M}_F$ , etc. The average across the face, for the BDDC deluxe algorithm, is then defined by

$$\bar{\mathbf{w}}_F := (S_F^{(i)} + S_F^{(j)})^{-1} (S_F^{(i)} \mathbf{w}_F^{(i)} + S_F^{(j)} \mathbf{w}_F^{(j)}).$$

We note that a more computationally efficient version of this averaging (scaling) can be obtained using approximate Schur complements as described in Section 6.

Instead of estimating  $(R_F^{(i)} \bar{\mathbf{w}}_F)^T S^{(i)} R_F^{(i)T} \bar{\mathbf{w}}_F$ , we can estimate the  $S^{(i)}$ -norm of  $R_F^{(i)T} (\mathbf{w}^{(i)} - \bar{\mathbf{w}}_F)$ . We easily find that

$$\mathbf{w}_F^{(i)} - \bar{\mathbf{w}}_F = (S_F^{(i)} + S_F^{(j)})^{-1} S_F^{(j)} (\mathbf{w}_F^{(i)} - \mathbf{w}_F^{(j)}).$$

By some more algebra, we find, after recalling that  $R_F^{(i)} S^{(i)} R_F^{(i)T} = S_F^{(i)}$ , that

$$\begin{aligned} & (R_F^T (\mathbf{w}_F^{(i)} - \bar{\mathbf{w}}_F))^T S^{(i)} (R_F^T (\mathbf{w}_F^{(i)} - \bar{\mathbf{w}}_F)) = \\ & (\mathbf{w}_F^{(i)} - \mathbf{w}_F^{(j)})^T S_F^{(j)} (S_F^{(i)} + S_F^{(j)})^{-1} S_F^{(i)} (S_F^{(i)} + S_F^{(j)})^{-1} S_F^{(j)} (\mathbf{w}_F^{(i)} - \mathbf{w}_F^{(j)}) \leq \\ & 2(\mathbf{w}_F^{(i)})^T S_F^{(j)} (S_F^{(i)} + S_F^{(j)})^{-1} S_F^{(i)} (S_F^{(i)} + S_F^{(j)})^{-1} S_F^{(j)} \mathbf{w}_F^{(i)} + \\ & 2(\mathbf{w}_F^{(j)})^T S_F^{(j)} (S_F^{(i)} + S_F^{(j)})^{-1} S_F^{(i)} (S_F^{(i)} + S_F^{(j)})^{-1} S_F^{(j)} \mathbf{w}_F^{(j)}. \end{aligned}$$

We can now prove two inequalities for the same left hand side:

$$S_F^{(j)} (S_F^{(i)} + S_F^{(j)})^{-1} S_F^{(i)} (S_F^{(i)} + S_F^{(j)})^{-1} S_F^{(j)} \leq S_F^{(i)}$$

and also

$$S_F^{(j)} (S_F^{(i)} + S_F^{(j)})^{-1} S_F^{(i)} (S_F^{(i)} + S_F^{(j)})^{-1} S_F^{(j)} \leq 1/4 S_F^{(j)}.$$

These bounds follow easily by considering the action of these operators on any eigenvector of the generalized eigenvalue problem  $S_F^{(i)} \phi = \lambda S_F^{(j)} \phi$  and just using that all its eigenvalues are strictly positive.

Thus, also writing down a bound for  $(R_F^{(j)} (\mathbf{w}_F^{(j)} - \bar{\mathbf{w}}_F))^T S^{(j)} R_F^{(j)T} (\mathbf{w}_F^{(j)} - \bar{\mathbf{w}}_F)$ , we find

$$\begin{aligned} & (R_F^{(i)T} (\mathbf{w}_F^{(i)} - \bar{\mathbf{w}}_F))^T S^{(i)} R_F^{(i)T} (\mathbf{w}_F^{(i)} - \bar{\mathbf{w}}_F) + (R_F^{(j)T} (\mathbf{w}_F^{(j)} - \bar{\mathbf{w}}_F))^T S^{(j)} R_F^{(j)T} (\mathbf{w}_F^{(j)} - \bar{\mathbf{w}}_F) \\ & \leq 2.5(\mathbf{w}_F^{(i)})^T S_F^{(i)} \mathbf{w}_F^{(i)} + 2.5(\mathbf{w}_F^{(j)})^T S_F^{(j)} \mathbf{w}_F^{(j)}. \end{aligned} \quad (2.8)$$

All that is now required are bounds which are local to individual subdomains, i.e., a bound of  $(\mathbf{w}_F^{(i)})^T S_F^{(i)} \mathbf{w}_F^{(i)}$  in terms of  $(\mathbf{w}^{(i)})^T S^{(i)} \mathbf{w}^{(i)}$ , etc. This observation is key

and allows us to derive estimates that work very well even for problems with a pair of material coefficients. We note that in our particular context, the primal constraints will not come into play for any face since these constraints are related to the subdomain edges only.

Each of the relevant equivalence classes, associated with the subdomain  $\Omega_i$ , will contribute to the value of  $E_D \mathbf{w}$ ; the contribution from the face  $F$  equals  $R_F^T \bar{\mathbf{w}}_F$ , where  $R_F$  is the restriction operator from  $\mathcal{M}_\Gamma$  to  $\mathcal{M}_F$ . These elements all belong to  $\widehat{W}$ .

We also need to consider averages across subdomain edges. We now introduce a restriction matrix  $R_E^{(i)}$  which maps the values on the interface  $\Gamma$  onto those on the element edges of  $E$ . If this subdomain edge is common to three subdomains  $\Omega_i, \Omega_j$ , and  $\Omega_k$ , the edge average  $\bar{\mathbf{w}}_E$  is defined by

$$\bar{\mathbf{w}}_E := (S_E^{(i)} + S_E^{(j)} + S_E^{(k)})^{-1} (S_E^{(i)} \mathbf{w}_E^{(i)} + S_E^{(j)} \mathbf{w}_E^{(j)} + S_E^{(k)} \mathbf{w}_E^{(k)}).$$

Here  $S_E^{(i)} := R_E^{(i)} S^{(i)} R_E^{(i)T}$ , etc.

By arguments similar to those for faces, we can show that

$$\begin{aligned} (R_E^{(i)T} (\mathbf{w}_E^{(i)} - \bar{\mathbf{w}}_E))^T S^{(i)} R_E^{(i)T} (\mathbf{w}_E^{(i)} - \bar{\mathbf{w}}_E) &\leq 3(\mathbf{w}_E^{(i)} - \mathbf{w}_{E\Pi})^T S_E^{(i)} (\mathbf{w}_E^{(i)} - \mathbf{w}_{E\Pi}) + \\ &3/4(\mathbf{w}_E^{(j)} - \mathbf{w}_{E\Pi})^T S_E^{(j)} (\mathbf{w}_E^{(j)} - \mathbf{w}_{E\Pi}) + 3/4(\mathbf{w}_E^{(k)} - \mathbf{w}_{E\Pi})^T S_E^{(k)} (\mathbf{w}_E^{(k)} - \mathbf{w}_{E\Pi}) \end{aligned} \quad (2.9)$$

Here  $\mathbf{w}_{E\Pi}$  is a restriction to the edge  $E$  of any element in the primal space. We can also develop similar bounds for any edge, common to more than three subdomains, using the same kinds of arguments; for some more details see [3].

The  $\tilde{S}$ -norm of the averaging operator  $E_D$  provides an estimate of the condition number of the BDDC algorithm:

$$\kappa(M_{BDDC}^{-1} \widehat{S}) \leq \|E_D\|_{\tilde{S}}^2. \quad (2.10)$$

This type of result has been known for a decade for the closely related FETI-DP algorithms; see [14]. For a detailed proof for BDDC algorithms, see, e.g., [18, Theorem 25]. The proof of a bound on  $\|E_D\|_{\tilde{S}}^2$  can be developed for one subdomain at a time, and each of these bounds is established by developing a good enough bound for each of the equivalence classes of the interface of the subdomain.

**3. Technical Tools.** We first collect four lemmas, Lemmas 4.16, 4.19, and variants of Lemmas 4.23 and 4.24, on  $W_{\text{grad}}^{h_i}$  from [23, Chap. 4]. We note that the proof of [23, Lemma 4.16] is not satisfactory and that we therefore include a complete proof of Lemma 3.1. We will use the abbreviation  $\omega_i := 1 + \log(H_i/h_i)$  and denote by  $I^h$  the standard nodal interpolation operator onto  $W_{\text{grad}}^{h_i}$ . All our norms are scaled with relative weights determined by the diameter of the subdomain. Thus,

$$\|u\|_{H^1(\Omega_i)}^2 := |u|_{H^1(\Omega_i)}^2 + H_i^{-2} \|u\|_{L^2(\Omega_i)}^2. \quad (3.1)$$

LEMMA 3.1.

$$\|u_h\|_{L^2(E)}^2 \leq C\omega_i \|u_h\|_{H^1(\Omega_i)}^2, \quad \forall u_h \in W_{\text{grad}}^{h_i},$$

and

$$\|u_h - \bar{u}_E\|_{L^2(E)}^2 \leq C\omega_i |u_h|_{H^1(\Omega_i)}^2, \quad \forall u_h \in W_{\text{grad}}^{h_i}.$$

Here  $\bar{u}_E$  is the average of  $u_h$  over the edge  $E$ . The same estimates also hold for any line segment that belongs to  $\Omega_i$ .

*Proof.* Our proof will be modeled on that of [1, Lemma 4.92], which provides a proof of a well-known finite element Sobolev inequality in two dimensions; cf. [23, Lemma 4.15] for a very different proof.

Let us consider a shape-regular tetrahedron  $T_E$  with a diameter on the order of  $H_i$  and which might be only a subset of  $\Omega_i$ . Consider the centroid  $c_K$  of any element  $K$  with at least one vertex on the edge  $E$  and construct a plane through this point with an intersection with  $T_E$  with a relatively large area  $\mathcal{A}_K$ . This can be accomplished by using only two sets of parallel planes. For  $c_K$ , we use a plane parallel to the face of  $T_E$  which intersects  $E$  only at the endpoint of  $E$  closest to  $c_K$ .

Inspecting the proof in [1], we see that the fact that the mesh on  $\mathcal{A}_K$ , inherited from the three dimensional mesh of  $T_E$ , can be quite irregular, with some very small elements, does not matter. What matters is that a sphere with a radius on the order of  $h$  and centered at  $c_K$  is contained in the element  $K$ . We can therefore use the two-dimensional finite element Sobolev inequality of [1, Lemma 4.92] to obtain the bound

$$|u_h(c_K)|^2 \leq C w_i \|u_h\|_{H^1(\mathcal{A}_K)}^2.$$

A bound of similar quality for  $u_h(x)$ ,  $x \in E \cap K$  can be obtained by also using [1, Lemma 4.5.3] to obtain

$$|u_h(x) - u_h(c_K)| \leq h_K |u_h|_{W_\infty^1(K)} \leq h_K^{-1/2} \|u_h\|_{H^1(K)}.$$

The proof of the first inequality is completed by estimating  $\sum_{x \in \mathcal{N}_E} h_K |u_h(x)|^2$ .

The proof of the second now follows from the first by using Poincaré's inequality.

Our arguments can also easily be extended to an arbitrary line segment.  $\square$

The following lemma has an elementary proof.

LEMMA 3.2. *Let  $\vartheta_E \in W_{grad}^{h_i}$  be the function which equals 1 at all nodes on  $E$  and vanishes at all other nodes of the closure of  $\Omega_i$ . Then,*

$$|I^h(\vartheta_E u_h)|_{H^1(\Omega_i)}^2 \leq C \|u_h\|_{L^2(E)}^2, \quad \forall u_h \in W_{grad}^{h_i}.$$

The following lemma has previously been established for triangular and rectangular subdomain faces.

LEMMA 3.3. *There exists a function  $\vartheta_F \in W_{grad}^{h_i}$ , which equals 1 at each node of a subdomain face  $F$ , which satisfies Assumption 1, of a subdomain and which vanishes at all other nodes of  $\partial\Omega_i$ , such that*

$$0 \leq \vartheta_F \leq 1, \quad \text{and} \quad |\nabla \vartheta_F| \leq C/r(x).$$

Here  $r(x)$  is the distance from  $x$  to  $\partial F$ .

*Proof.* This result is established by explicitly constructing a function, with these boundary values, and then estimating its gradient. We will use similar techniques when establishing a new technical tool in Lemma 3.5.

For each subdomain edge  $E$  of the face  $F$ , we construct a tetrahedron  $T_E$  with a triangular base defined by  $E$  and the special point  $c_F$  of Assumption 1.  $T_E$  also has a vertex  $V$  located on the normal, through  $c_F$ , to the face and at a distance on the order of  $H_i$  from  $c_F$ . In case  $F$  is not planar, we will use an average of the normal vectors of the triangles which define  $F$ . We also assume that  $T_E \subset \Omega_i$ .

For each  $T_E$ , we now introduce a cylindrical coordinate system,  $(r, \theta, z)$ , with  $r$  the distance from the edge  $E$  and the  $z$ -axis along  $E$ . The angular variable  $0 \leq \theta \leq \theta_E$  is 0 on the face of  $T_E$  defined by  $E$  and  $V$ , while  $\theta = \theta_E$  on the face  $F$ .

We now construct the function  $\vartheta_F$  which is constant on each plane through the edge  $E$  and defined by its values on the line segment between  $c_F$  and  $V$ . It equals 1 at  $c_F$  and decreases linearly along the line segment to the value 0 at the vertex  $V$ . The resulting function is not well defined on  $\partial F$  but is otherwise continuous in all of  $\Omega_i$  once that its value is set to 0 outside the tetrahedra  $T_E$ . We finally let  $\vartheta_F$  vanish on the boundary  $\partial F$  of the face  $F$  and replace this function by its piece-wise linear interpolant. The bound of the lemma can now easily be established.  $\square$

No new ideas are now required to modify the proof of [23, Lemma 4.24] for the more general subdomain faces allowed by Assumption 1.

LEMMA 3.4. *Let  $\vartheta_F$  be the function defined in Lemma 3.3 for a subdomain face satisfying Assumption 1. Then,*

$$|I^h(\vartheta_F u_h)|_{H^1(\Omega_i)}^2 \leq C\omega_i^2 \|u_h\|_{H^1(\Omega_i)}^2, \quad \forall u_h \in W_{grad}^{h_i}. \quad (3.2)$$

The next lemma is of crucial importance to our theory and is believed to be new. It allows us to obtain a good estimate of certain elements of  $W_{curl}^{h_i}$ , obtained by zeroing out the Nédélec coefficients on the boundary of a face  $F$  and on the faces adjacent to  $F$ .

LEMMA 3.5. *Let  $F$  be a subdomain face, of the polyhedron  $\Omega_i$ , which satisfies Assumption 1. Further, let  $f_{\partial F} \in W_{grad}^{h_i}$  have vanishing nodal values everywhere in  $\Omega_i$  except on  $\partial F$ . There then exists a  $\mathbf{g}_{iF} \in W_{curl}^{h_i}$  such that  $\lambda_e(\mathbf{g}_{iF}) = \lambda_e(\nabla f_{\partial F}), \forall e \in \mathcal{M}_{F_b}$ ,  $\lambda_e(\mathbf{g}_{iF}) = 0$  for all other element edges of  $\Gamma_i$ , and*

$$\|\mathbf{g}_{iF}\|_{L^2(\Omega_i)}^2 \leq C(\omega_i \|f_{\partial F}\|_{L^2(\partial F)}^2 + H_i^2 \|\nabla f_{\partial F} \cdot \mathbf{t}_{\partial F}\|_{L^2(\partial F)}^2), \quad (3.3)$$

$$\|\nabla \times \mathbf{g}_{iF}\|_{L^2(\Omega_i)}^2 \leq C\omega_i \|\nabla f_{\partial F} \cdot \mathbf{t}_{\partial F}\|_{L^2(\partial F)}^2. \quad (3.4)$$

*Proof.* In the proof of this lemma, we will construct two functions  $\nabla f_{iF}^h$  and  $\mathbf{f}_{iF}^h$  such that  $\mathbf{g}_{iF} := \nabla f_{\partial F} - \nabla f_{iF}^h + \mathbf{f}_{iF}^h$  has the desired properties. The need for these two functions became apparent when initial attempts to prove the lemma by directly estimating the contributions from the edges of  $\mathcal{M}_{F_b}$  were unsuccessful.

We note that both  $\nabla f_{\partial F}$  and  $\nabla f_{iF}^h$  are curl-free, and thus  $\nabla \times \mathbf{g}_{iF} = \nabla \times \mathbf{f}_{iF}^h$ . The nodal values of  $f_{iF}^h \in W_{grad}^{h_i}$  are chosen to be identical to those of  $f_{\partial F}$  along  $\partial F$  and to vanish at all other nodes on  $\Gamma_i$  not in the closure of  $F$ . Thus,  $\lambda_e(\nabla f_{\partial F} - \nabla f_{iF}^h) = 0, \forall e \in \mathcal{M}_{\Gamma_i} \setminus \mathcal{M}_F$ . The function  $\mathbf{f}_{iF}^h \in W_{curl}^{h_i}$  will have  $\lambda_e(\mathbf{f}_{iF}^h) = 0$  for the same set of element edges while  $\lambda_e(\mathbf{f}_{iF}^h) = \lambda_e(\nabla f_{iF}^h), \forall e \in \mathcal{M}_F$ .

We will develop estimates consistent with those of the lemma for each of the three functions, which define  $\mathbf{g}_{iF}$ , separately. We first consider the given function  $f_{\partial F} \in W_{grad}^{h_i}$  which has vanishing nodal values in the closure of  $\Omega_i$  except on  $\partial F$ . By Lemma 3.2, we have

$$\|\nabla f_{\partial F}\|_{L^2(\Omega_i)}^2 \leq C \|f_{\partial F}\|_{L^2(\partial F)}^2. \quad (3.5)$$

We start our construction of the other two functions by triangulating the face  $F$  into long triangles. Each of them has two vertices at two consecutive nodes on  $\partial F$  and a third at  $c_F$ , the centroid of  $F$ . We then introduce a continuous, piecewise linear

function defined on  $F$ , call it  $f_F$ , using the nodal values of  $f_{\partial F}$  at the nodes on  $\partial F$  and  $\bar{f}_{\partial F}$ , the average of  $f_{\partial F}$  over  $\partial F$ , at  $c_F$ . The motivating goal here is to obtain a function that is identical to  $f_{\partial F}$  along  $\partial F$ , but does not change as rapidly near  $\partial F$  in the direction orthogonal to  $\partial F$ .

The long triangles just introduced can naturally be regarded as subsets of larger triangles each with a side equal to a subdomain edge  $E$  and with a vertex at  $c_F$ . We will construct a function  $f_{iF}$  on the set of tetrahedra  $T_E$ , introduced in the proof of Lemma 3.3, each with one of these larger triangles as a base.

For the tetrahedron  $T_E$  associated with the edge  $E$ , we introduce two coordinate systems. The first one is Cartesian,  $(x, y, z)$ , with the  $x$ -axis orthogonal to  $E$  and in the plane of  $F$ , the  $y$ -axis parallel to the normal of  $F$ , and the  $z$ -axis along  $E$ . The second one is the cylindrical coordinate system,  $(r, \theta, z)$ , as in the proof of Lemma 3.3, with  $r$  being the distance from the edge  $E$  and the  $z$ -axis again along  $E$ . The angular variable  $0 \leq \theta \leq \theta_E$  is 0 on the face of  $T_E$  defined by  $E$  and  $V$ , while  $\theta = \theta_E$  on the face  $F$ .

We now construct a function  $f_{iF}(x, y, z)$ , which equals  $f_F$  on the closure of the face  $F$  and which vanishes on the rest of the boundary of the union of the closures of the tetrahedra  $T_E$  and in the rest of the subdomain. For the tetrahedra  $T_E$ , this function is a product of  $f_F$  and a function  $\phi_E(\theta)$  which is constant on each plane through the edge  $E$  and defined by its values on the line segment between  $c_F$  and  $V$ . The value of  $\phi_E(\theta)$  equals 1 at  $c_F$  and its values decreases linearly to 0 at the vertex  $V$ . The resulting function is not well defined on  $\partial F$  but is otherwise continuous in all of  $\Omega_i$  once that  $f_{iF}(x, y, z)$  is set to 0 outside the tetrahedra  $T_E$ .

On  $\partial F$ , we set  $f_{iF} = f_F$ . We finally obtain the function  $f_{iF}^h \in W_{\text{grad}}^{h_i}$  by interpolating:

$$f_{iF}^h(x, y, z) := I^{h_i}(f_{iF}(x, y, z)).$$

The next task is to estimate the gradient of  $f_{iF}(x, y, z)$ ; once we have done so, we can use the fact that for each element  $K$ ,

$$|\nabla I^h(f_{iF})| \leq C \max_{x \in K} |\nabla f_{iF}|.$$

We first compute the derivatives of  $f_F(x, z)$  with respect to  $x$  and  $z$  for one long triangle at a time. Since  $f_F = f_{\partial F}$  along  $\partial F$  and the derivative with respect to  $z$  constant, we have

$$|\partial f_F / \partial z|^2 = |\nabla f_{\partial F} \cdot \mathbf{t}_{\partial F}|^2. \quad (3.6)$$

The square of the derivative of  $f_F$  with respect to  $x$  can, after considering the simple geometry, be bounded by

$$|\partial f_F / \partial x|^2 \leq C(|\nabla f_{\partial F} \cdot \mathbf{t}_{\partial F}|^2 + H_i^{-2}(|f_{\partial F_{e_1}} - \bar{f}_{\partial F}|^2 + |f_{\partial F_{e_2}} - \bar{f}_{\partial F}|^2)), \quad (3.7)$$

where  $f_{\partial F_{e_1}}$  and  $f_{\partial F_{e_2}}$  are the values at the endpoints of the element edge, on  $\partial F$ , of the long triangle. When we add the contributions from all the long triangles, we can use the Poincaré inequality and conclude that

$$\|f_{\partial F} - \bar{f}_{\partial F}\|_{L^2(\partial F)} \leq CH_i \|\nabla f_{\partial F} \cdot \mathbf{t}_F\|_{L^2(\partial F)}$$

Finally, it is easy to prove that  $|\nabla \phi_E(\theta)| \leq C/r$ .

Integrating  $|\nabla f_{iF}^h|^2$  over  $T_E$  using cylindrical coordinates, while excluding all elements of the triangulation which touch  $E$ , summing over all subdomain edges of  $\partial F$ , and using the Cauchy-Schwarz inequality gives us

$$\|\nabla f_{iF}^h\|_{L^2(\Omega_i \setminus \Omega_{i\partial F})}^2 \leq C(H_i^2 \|\nabla f_{\partial F} \cdot \mathbf{t}_{\partial F}\|_{L^2(\partial F)}^2 + \omega_i \|f_{\partial F}\|_{L^2(\partial F)}^2), \quad (3.8)$$

where  $\Omega_{i\partial F}$  is the union of all elements in  $\Omega_i$  that touch  $\partial F$ . From elementary estimates, we also obtain

$$\|\nabla f_{iF}^h\|_{L^2(\Omega_{i\partial F})}^2 \leq C(h_i^2 \|\nabla f_{\partial F} \cdot \mathbf{t}_{\partial F}\|_{L^2(\partial F)}^2 + \|f_{\partial F}\|_{L^2(\partial F)}^2). \quad (3.9)$$

We next construct an edge finite element function  $\mathbf{f}_{iF}^h \in W_{\text{curl}}^{h_i}$  with the same tangential data as  $\nabla f_{iF}^h$  for all the edges of  $F$ , while vanishing along  $\partial F$  and on all other edges of  $\Gamma_i$ . To this end, we first define

$$\tilde{\mathbf{f}}_{iF}^h := \Pi^{h_i}(\nabla f_F(x, z)) = \sum_{e \in \mathcal{M}_{\bar{\Omega}_i}} \lambda_e(\nabla f_F) \mathbf{N}_e,$$

where  $\mathcal{M}_{\bar{\Omega}_i}$  is the set of all finite element edges in the closure of  $\Omega_i$ . Here,  $f_F$  is defined for the three-dimensional space by making it constant as a function of  $y$ . Notice that the curl of  $\tilde{\mathbf{f}}_{iF}^h$  vanishes since it is the finite element interpolant of a gradient. Again, looking at one tetrahedron at a time, we next define

$$\mathbf{f}_{iF}^h := \sum_{e \in \mathcal{M}_{\bar{\Omega}_i} \setminus \mathcal{M}_{\partial F}} \phi(\theta_e) \lambda_e(\nabla f_F) \mathbf{N}_e,$$

where  $\theta_e$  is the value of  $\theta$  at the center of edge  $e$ . The restriction of the function  $\phi$  to the tetrahedron  $T_E$  equals  $\phi_E$  and the value of  $\theta_e$  refers to that of the cylindrical coordinate system of  $T_E$ . Similarly to what was done for  $f_{iF}$ , we have set  $\lambda_e(\mathbf{f}_{iF}^h) = 0$  in all parts of  $\Omega_i$  outside all the tetrahedra. Notice that since  $\phi(\theta) = 1$  on  $F$  that  $\lambda_e(\mathbf{f}_{iF}^h) = \lambda_e(\nabla f_{iF}^h)$  for all  $e \in \mathcal{M}_F$  and  $\lambda_e(\mathbf{f}_{iF}^h) = 0$  for all remaining edges of  $\Gamma_i$ .

Using (3.6) and (3.7),  $|\phi(\theta)| \leq 1$ , and (2.1) gives us

$$\|\mathbf{f}_{iF}^h\|_{L^2(\Omega_i)}^2 \leq CH_i^2 \|\nabla f_{\partial F} \cdot \mathbf{t}_f\|_{L^2(\partial F)}^2. \quad (3.10)$$

We next obtain an estimate for the curl of  $\mathbf{f}_{iF}^h$ . Considering an individual element  $K$  and the definition of  $\mathbf{f}_{iF}^h$ , we have

$$\mathbf{f}_{iF}^h = \phi_K \tilde{\mathbf{f}}_{iF}^h + \sum_{e \in \mathcal{M}_K} (\phi(\theta_e) - \phi_K) \lambda_e(\nabla f_F) \mathbf{N}_e, \quad (3.11)$$

where  $\phi_K$  is the value of  $\phi(\theta)$  at the centroid of  $K$  and  $\mathcal{M}_K$  is the set of edges for  $K$ . Since the curl of the first term on the right-hand-side of (3.11) vanishes, it follows from (2.2) and

$$\|\phi(\theta) - \phi_K\|_{L^\infty(K)} \leq Ch_K/r_K$$

that

$$\|\nabla \times \mathbf{f}_{iF}^h\|_{L^\infty(K)}^2 \leq (C/r_K^2) \|\nabla f_F\|_{L^\infty(K)}^2, \quad (3.12)$$

where  $h_K$  is the diameter of  $K$  and  $r_K$  is the value of  $r$  at the centroid of  $K$ . Similar to what was done to obtain the estimate in (3.8), we use cylindrical coordinates to

sum the estimate in (3.12) for all elements not touching  $\partial F$ . Combining this result with an estimate for elements touching  $\partial F$  obtained using (3.6), (3.7), and (2.2), we find

$$\|\nabla \times \mathbf{f}_{iF}^h\|_{L^2(\Omega_i)}^2 \leq C\omega_i \|\nabla f_{\partial F} \cdot \mathbf{t}_{\partial F}\|_{L^2(\partial F)}^2. \quad (3.13)$$

With  $\mathbf{g}_{iF} := \nabla f_{\partial F} - \nabla f_{iF}^h + \mathbf{f}_{iF}^h$ , we see by construction that  $\lambda_e(\mathbf{g}_{iF}) = \lambda_e(\nabla f_{\partial F})$  for all  $e \in \mathcal{M}_{F_b}$  and  $\lambda_e(\mathbf{g}_{iF}) = 0$  for all other edges of  $\partial\Omega_i$ . The estimate in (3.3) now follows directly from (3.5), (3.8), (3.9), and (3.10), while (3.4) follows from (3.13) since  $\nabla \times \mathbf{g}_{iF} = \nabla \times \mathbf{f}_{iF}^h$ .  $\square$

REMARK 2. *We note that in an earlier, much longer proof, a bound as in (3.4) without the factor  $\omega_i$  has been established. However, this factor for one term of our bound, does not have any effect on our final condition number estimate.*

We finally recall a result from Hiptmair and Xu [8, Lemma 5.1]. We note that paper was preceded by [7], with a similar lemma applied to an iterative method quite different from ours.

LEMMA 3.6. *For any polyhedral subdomain  $\Omega_i$  and any  $\mathbf{w}_i \in W_{curl}^{h_i}$ , there is a  $\mathbf{q}_i \in W_{curl}^{h_i}$ ,  $\Psi_i \in (W_{grad}^{h_i})^3$ , and  $p_i \in W_{grad}^{h_i}$  such that*

$$\mathbf{w}_i = \mathbf{q}_i + \Pi^{h_i}(\Psi_i) + \nabla p_i, \quad (3.14)$$

$$\|\nabla p_i\|_{L^2(\Omega_i)}^2 \leq C(\|\mathbf{w}_i\|_{L^2(\Omega_i)}^2 + H_i^2 \|\nabla \times \mathbf{w}_i\|_{L^2(\Omega_i)}^2), \quad (3.15)$$

$$\|h_i^{-1} \mathbf{q}_i\|_{L^2(\Omega_i)}^2 + \|\Psi_i\|_{H^1(\Omega_i)}^2 \leq C \|\nabla \times \mathbf{w}_i\|_{L^2(\Omega_i)}^2. \quad (3.16)$$

We note that

$$\|\Psi_i\|_{L^2(\Omega_i)}^2 \leq CH_i^2 \|\nabla \times \mathbf{w}_i\|_{L^2(\Omega_i)}^2 \quad (3.17)$$

follows directly from (3.16) and (3.1).

**4. The Main Result.** In this section, we will obtain bounds for the right hand sides of (2.9) and (2.8), and thus complete the proof of our main result:

THEOREM 4.1. *The BDDC preconditioned operator for Algorithm B has a condition number bound of*

$$\kappa(M^{-1}A) \leq C\omega^2 \min(\eta, (H/h)^2), \quad (4.1)$$

where  $\omega := \max_i \omega_i$ ,  $\eta := \max_i \eta_i$ , where  $\eta_i := 1 + \beta_i H_i^2 / \alpha_i$ , and  $H/h := \max_i H_i / h_i$ .

**4.1. Edge Analysis.** In this subsection, we will develop estimates related to the subdomain edges, in particular, an estimate of  $\mathbf{w}_i - \mathbf{w}_{E\Pi}$ , which can then be combined with formula (2.9).

Let  $E$  denote a subdomain edge common to  $\Omega_i$  and  $\Omega_k$  as well as to other subdomains. With reference to (2.4) and the decomposition in (3.14), we have along  $E$

$$a_E(\mathbf{w}_i) + \nabla \phi_{iE} \cdot \mathbf{t}_e = (\mathbf{s}_i + \nabla p_i) \cdot \mathbf{t}_e, \quad (4.2)$$

where  $\mathbf{s}_i := \mathbf{q}_i + \Pi^{h_i}(\Psi_i)$ . Integration of (4.2) gives

$$p_i(s) = \bar{p}_{iE} + \phi_{iE}(s) - \bar{\phi}_{iE} - \int_{-|E|/2}^s \mathbf{s}_i \cdot \mathbf{t}_e ds + a_E(\mathbf{w}_i)s + \bar{s}_i, \quad (4.3)$$

where  $\bar{p}_{iE}$  is the average of  $p_i$  over  $E$ ,  $\bar{\phi}_{iE}$  that of  $\phi_{iE}$ , and

$$\bar{s}_i = 1/|E| \int_{-|E|/2}^{|E|/2} \int_{-|E|/2}^s \mathbf{s}_i \cdot \mathbf{t}_e d\tilde{s} ds. \quad (4.4)$$

(We can easily check that the average of the right hand side of (4.3) over  $E$  equals  $\bar{p}_{iE}$  as required.)

By (2.9), and the two primal constraints,  $\bar{\phi}_{iE} = \bar{\phi}_{kE}$  and  $a_E(\mathbf{w}_i) = a_E(\mathbf{w}_k)$ , we only need to estimate the  $S^{(i)}$ -norm of the dual part of  $\mathbf{w}_i \cdot \mathbf{t}_e$  given by  $\nabla \phi_{i\Delta} \cdot \mathbf{t}_e$  where

$$\phi_{i\Delta} = p_i - \bar{p}_{iE} - \bar{s}_i + \int_{-|E|/2}^s \mathbf{s}_i \cdot \mathbf{t}_e ds. \quad (4.5)$$

From the triangle and Cauchy-Schwarz inequalities, we then find that

$$|\phi_{i\Delta}| \leq |p_i - \bar{p}_{iE}| + 2|E|^{1/2} \|\mathbf{s}_i\|_{L^2(E)}. \quad (4.6)$$

We can estimate the  $L^2(E)$ -norm of the first term by using Lemma 3.1 and (3.15). Using the estimate of (3.16) and again applying Lemma 3.1, we then find that

$$\|\mathbf{s}_i\|_{L^2(E)}^2 \leq C\omega_i \|\nabla \times \mathbf{w}_i\|_{L^2(\Omega_i)}^2. \quad (4.7)$$

Thus,

$$\begin{aligned} \beta_i \|\nabla \phi_{i\Delta}\|_{L^2(\Omega_i)}^2 &\leq C\beta_i \|\phi_{i\Delta}\|_{L^2(E)}^2 \\ &\leq C\omega_i (\beta_i \|\mathbf{w}_i\|_{L^2(\Omega_i)}^2 + \beta_i H_i^2 \|\nabla \times \mathbf{w}_i\|_{L^2(\Omega_i)}^2). \end{aligned} \quad (4.8)$$

We can now easily express the right hand side of this estimate in terms of

$$E_i(\mathbf{w}_i) = \alpha_i \|\nabla \times \mathbf{w}_i\|_{L^2(\Omega_i)}^2 + \beta_i \|\mathbf{w}_i\|_{L^2(\Omega_i)}^2$$

and the factor  $\eta_i$ .

We note that the resulting estimate has one fewer  $\omega_i$  factors than the related estimate [22, (8.4)]. In summary, we get a single factor of  $\omega_i$  when estimating the edge components. Since  $\|\nabla \times \mathbf{w}_i\|_{L^2(\Omega_i)} \leq Ch_i^{-1} \|\mathbf{w}_i\|_{L^2(\Omega_i)}$ , we see that our estimate can be generalized slightly to read

$$E_i(\nabla(\phi_{i\Delta})) \leq C\omega_i \min(\eta_i, (H_i/h_i)^2) E_i(\mathbf{w}_i). \quad (4.9)$$

**4.2. Face Analysis.** We next turn to an estimate of the face components of the decomposition of our finite element functions defined on the interface  $\Gamma_i$ . All we need to do is to estimate one of the terms of the right hand side of (2.8).

We will no longer work with the edge averages  $a_E(\mathbf{w}_i)$ , for which no satisfactory estimates can be developed. Instead, following Toselli [22, Sect. 7], we will work with an average  $a_{\partial F}(\mathbf{w}_i)$  over the boundary of the face  $F$ . The average circulation of  $\mathbf{w}_i$  about  $\partial F$  is defined, as on [22, page 121], by

$$a_{\partial F}(\mathbf{w}_i) := |\partial F|^{-1} \int_{\partial F} \mathbf{w}_i \cdot \mathbf{t}_{\partial F} ds,$$

where  $\mathbf{t}_{\partial F}$  is a unit tangent vector along  $\partial F$ . Decomposing  $\mathbf{w}_i$  according to (3.14) and noting that  $a_{\partial F}(\nabla p_i) = 0$ , we find that

$$a_{\partial F}(\mathbf{w}_i) = |\partial F|^{-1} \int_{\partial F} \mathbf{s}_i \cdot \mathbf{t}_{\partial F} ds,$$

and by using the estimate for  $\|\mathbf{s}_i\|_{L^2(E)}$  given in (4.7), that

$$|a_{\partial F}(\mathbf{w}_i)|^2 \leq CH_i^{-1} \omega_i \|\nabla \times \mathbf{w}_i\|_{L^2(\Omega_i)}^2. \quad (4.10)$$

We note that this estimate has one fewer factors of  $\omega_i$  than in [22, Lemma 7.5]. A comment following that lemma suggests that an estimate the same as ours already is available in the proof of [24, Lemma 4.1].

Returning to the decomposition in (3.14), we have on  $\partial F$

$$\mathbf{w}_i - a_{\partial F}(\mathbf{w}_i)\Phi_{\partial F} = \nabla p_i + (\mathbf{s}_i - a_{\partial F}(\mathbf{w}_i)\Phi_{\partial F}), \quad (4.11)$$

where  $\Phi_{\partial F} = \sum_{E \subset \partial F} \Phi_E$ . We note that the average circulation of the term in parenthesis on the right hand side of (4.11) vanishes. Thus, there is a nodal function  $\tilde{p}_{i\partial F}$ , which vanishes except at the nodes on  $\partial F$ , such that for  $e \in \partial F$

$$\nabla \tilde{p}_{i\partial F} \cdot \mathbf{t}_e = (\mathbf{s}_i - a_{\partial F}(\mathbf{w}_i)\Phi_{\partial F}) \cdot \mathbf{t}_e. \quad (4.12)$$

From (4.11), we thus have for  $e \in \partial F$ ,

$$\mathbf{w}_i \cdot \mathbf{t}_e = a_{\partial F}(\mathbf{w}_i) + (\nabla p_{i\partial F} + \nabla \tilde{p}_{i\partial F}) \cdot \mathbf{t}_e, \quad (4.13)$$

where  $\tilde{p}_{i\partial F} := \sum_{n \in \mathcal{N}_{\partial F}} \tilde{p}_i(n) \phi_n$ , with  $\tilde{p}_i(n)$  the value of  $\tilde{p}_i$  at node  $n$ , and  $\phi_n$  the nodal basis function for node  $n$ . Integration of (4.12) along  $\partial F$  for  $0 < s < |\partial F|$  and choosing  $\tilde{p}_{i\partial F}(0) = 0$  gives

$$\tilde{p}_{i\partial F}(s) = -a_{\partial F}(\mathbf{w}_i)s + \int_0^s (\mathbf{s}_i \cdot \mathbf{t}_{\partial F}) ds. \quad (4.14)$$

From the estimates in (4.10), (3.16), the Cauchy-Schwarz inequality, and Lemma 3.1, we obtain

$$|\tilde{p}_{i\partial F}|^2 \leq CH_i \omega_i \|\nabla \times \mathbf{w}_i\|_{L^2(\Omega_i)}^2, \quad (4.15)$$

and thus by Lemma 3.2,

$$\|\nabla \tilde{p}_{i\partial F}\|_{L^2(\Omega_i)}^2 \leq CH_i^2 \omega_i \|\nabla \times \mathbf{w}_i\|_{L^2(\Omega_i)}^2. \quad (4.16)$$

Comparing the decomposition in (2.4) with (4.13), it follows that on  $\partial F$

$$\mathbf{w}_{i\partial F} := \mathbf{w}_i = \sum_{E \subset \partial F} (a_E(\mathbf{w}_i)\Phi_E + \nabla \phi_{iE}) = a_{\partial F}(\mathbf{w}_i)\Phi_{\partial F} + \nabla p_{i\partial F} + \nabla \tilde{p}_{i\partial F}. \quad (4.17)$$

We now obtain the contribution  $\mathbf{w}_{iF}$  from the face by subtracting the function  $\mathbf{w}_{i\partial F}$ , attributed to the boundary of the face, from  $\mathbf{w}_i$ . Thus, we see that since  $\Phi_{\partial F}$  vanishes on  $F$

$$\mathbf{w}_{iF} \cdot \mathbf{t}_e = (\mathbf{w}_i - \nabla p_{i\partial F} - \nabla \tilde{p}_{i\partial F}) \cdot \mathbf{t}_e \quad \forall e \in \mathcal{M}_F.$$

The present goal is to obtain estimates for a function  $\tilde{\mathbf{w}}_{iF}$  with the same boundary data as  $\mathbf{w}_{iF}$  on  $F$ , namely,

$$\lambda_e(\tilde{\mathbf{w}}_{iF}) = \begin{cases} \lambda_e(\mathbf{w}_{iF}) & \text{for } e \in \mathcal{M}_F \\ 0 & \text{for } e \in \mathcal{M}_{\partial\Omega_i} \setminus \mathcal{M}_F. \end{cases} \quad (4.18)$$

We note that a bound of the energy of any function with this boundary data will provide an upper bound for  $(\mathbf{w}_F^{(i)})^T S_F^{(i)} \mathbf{w}_F^{(i)}$  as required. With this in mind, we define  $\mathbf{r}_{iF}$  to be the function  $\mathbf{g}_{iF}$  of Lemma 3.5 for  $f_{\partial F} = \tilde{p}_{i\partial F}$ . From (4.12), (4.10), and (3.16), we obtain

$$\|\nabla \tilde{p}_{i\partial F} \cdot \mathbf{t}_{\partial F}\|_{L^2(\partial F)}^2 \leq C\omega_i \|\nabla \times \mathbf{w}_i\|_{L^2(\Omega_i)}^2, \quad (4.19)$$

and then find from (4.15) and Lemma 3.5 that

$$\|\mathbf{r}_{iF}\|_{L^2(\Omega_i)}^2 \leq CH_i^2 \omega_i^2 \|\nabla \times \mathbf{w}_i\|_{L^2(\Omega_i)}^2, \quad (4.20)$$

$$\|\nabla \times \mathbf{r}_{iF}\|_{L^2(\Omega_i)}^2 \leq C\omega_i^2 \|\nabla \times \mathbf{w}_i\|_{L^2(\Omega_i)}^2. \quad (4.21)$$

We note that, by construction,

$$\lambda_e(\mathbf{r}_{iF}) = \begin{cases} \lambda_e(\nabla \tilde{p}_{i\partial F}) & \text{for } e \in \mathcal{M}_F \\ 0 & \text{for } e \in \mathcal{M}_{\partial\Omega_i} \setminus \mathcal{M}_F. \end{cases} \quad (4.22)$$

We next obtain estimates related to the various terms in the decomposition of  $\mathbf{w}_i$  given by (3.14). We will use the function  $\vartheta_F$  of Lemmas 3.3 and 3.4 and define  $\Psi_{iF} := \Pi^{h_i}(I^{h_i}(\vartheta_F \Psi))$ . We find from (3.17),  $0 \leq \vartheta_F \leq 1$ , (3.16), (3.2), and standard estimates for edge element interpolations that

$$\|\Psi_{iF}\|_{L^2(\Omega_i)}^2 \leq CH_i^2 \|\nabla \times \mathbf{w}_i\|_{L^2(\Omega_i)}^2, \quad (4.23)$$

$$\|\nabla \times \Psi_{iF}\|_{L^2(\Omega_i)}^2 \leq C\omega_i^2 \|\nabla \times \mathbf{w}_i\|_{L^2(\Omega_i)}^2. \quad (4.24)$$

Let  $\vartheta_{W_i}$  denote a nodal function which is 1 at all subdomain edges and vertices of  $\Omega_i$  and 0 at all other nodes of  $\Omega_i$ . We next define a function in  $W_{\text{curl}}^{h_i}$  by  $\Psi_{i\partial F} := \sum_{e \in \mathcal{M}_F} \lambda_e(\Psi_{W_i}) \mathcal{N}_e$  where  $\Psi_{W_i} := \Pi^{h_i}(I^{h_i}(\vartheta_{W_i} \Psi))$ . From (2.1) and (3.17), we find that

$$\|\Psi_{i\partial F}\|_{L^2(\Omega_i)}^2 \leq C \sum_{e \in \mathcal{M}_F} h_i^3 \lambda_e^2(\Psi_{i\partial F}) \leq C \|\Psi_i\|_{L^2(\Omega_i)}^2 \leq CH_i^2 \|\nabla \times \mathbf{w}_i\|_{L^2(\Omega_i)}^2, \quad (4.25)$$

and from (2.2), Lemma 3.1, and (3.16), that

$$\|\nabla \times \Psi_{i\partial F}\|_{L^2(\Omega_i)}^2 \leq C\omega_i \|\nabla \times \mathbf{w}_i\|_{L^2(\Omega_i)}^2. \quad (4.26)$$

For  $\mathbf{q}_{iF} := \sum_{e \in \mathcal{M}_F} \lambda_e(\mathbf{q}_i) \mathcal{N}_e$ , we find from elementary estimates and (3.16) that

$$\begin{aligned} \|\mathbf{q}_{iF}\|_{L^2(\Omega_i)}^2 &\leq C \sum_{e \in \mathcal{M}_F} h_i^3 \lambda_e^2(\mathbf{q}_i) \leq C \|\mathbf{q}_i\|_{L^2(\Omega_i)}^2 \\ &\leq Ch_i^2 \|\nabla \times \mathbf{w}_i\|_{L^2(\Omega_i)}^2 \leq C \|\mathbf{w}_i\|_{L^2(\Omega_i)}^2, \end{aligned} \quad (4.27)$$

$$\|\nabla \times \mathbf{q}_{iF}\|_{L^2(\Omega_i)}^2 \leq C \sum_{e \in \mathcal{M}_F} h_i \lambda_e^2(\mathbf{q}_i) \leq C \|h_i^{-1} \mathbf{q}_i\|_{L^2(\Omega_i)}^2 \leq C \|\nabla \times \mathbf{w}_i\|_{L^2(\Omega_i)}^2. \quad (4.28)$$

Defining  $p_{iF} := I^{h_i}(\vartheta_F p_i)$  and choosing the mean of  $p_i$  over  $\Omega_i$  to vanish, it follows from (3.15), (3.2), and Lemma 3.4 that

$$\|\nabla p_{iF}\|_{L^2(\Omega_i)}^2 \leq C\omega_i^2 (\|\mathbf{w}_i\|_{L^2(\Omega_i)}^2 + H_i^2 \|\nabla \times \mathbf{w}_i\|_{L^2(\Omega_i)}^2), \quad (4.29)$$

We note that  $p_{iF} = p_i - p_{i\partial F}$ . For

$$\tilde{\mathbf{g}}_{iF} := \Psi_{iF} + \Psi_{i\partial F} + \mathbf{q}_{iF} + \nabla p_{iF},$$

we find from the estimates in (4.23-4.29) that

$$E_i(\tilde{\mathbf{g}}_{iF}) \leq C\omega_i^2 E_i(\mathbf{w}_i), \quad (4.30)$$

and, by construction, that

$$\lambda_e(\tilde{\mathbf{g}}_{iF}) = \begin{cases} \lambda_e(\mathbf{w}_i - \nabla p_{i\partial F}) & \text{for } e \in \mathcal{M}_F \\ 0 & \text{for } e \in \mathcal{M}_{\partial\Omega_i} \setminus \mathcal{M}_F. \end{cases} \quad (4.31)$$

We now choose

$$\tilde{\mathbf{w}}_{iF} = \tilde{\mathbf{g}}_{iF} - \mathbf{r}_{iF}, \quad (4.32)$$

and can confirm from (4.31), (4.2), and (4.22), that  $\tilde{\mathbf{w}}_{iF}$  satisfies (4.18). In other words,  $\tilde{\mathbf{w}}_i$  has the same boundary values as  $\mathbf{w}_i$  on  $F$ .

From the estimates in (4.30), (4.16), (4.20), (4.21), and noting that  $E_i(\mathbf{w}_{iF}) \leq E_i(\tilde{\mathbf{w}}_{iF})$ , we find

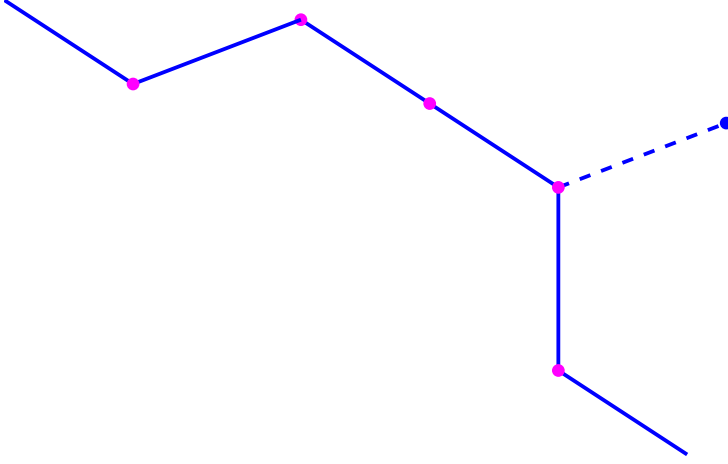
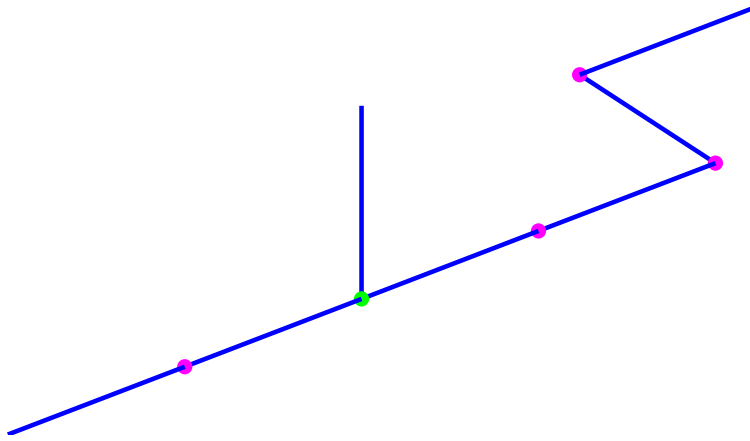
$$E_i(\mathbf{w}_{iF}) \leq C\omega_i^2 \min(\eta_i, (H_i/h_i)^2) E_i(\mathbf{w}_i). \quad (4.33)$$

**5. Implementation Details.** In the course of generating numerical results for irregular-shaped subdomains (see Table 6.4), it became apparent that certain care must be taken in the specification of subdomain edges. Namely, the simple definition of a subdomain edge consisting of all the element edges shared by the same set of three or more subdomains is not always sufficient. Specifically, we identified three different cases where this definition led to problems. The good news is that a simple solution was identified for each of these cases.

The first problematic case is when a subdomain edge consists of two or more disconnected components. Here we say that two edges of a subdomain edge are connected if they have a single endpoint node in common. Notice for two or more components that the subdomain edge will have more than two endpoints. The solution in this case is to simply treat each of the components as a separate subdomain edge. We note that this practice has also been used previously for scalar elliptic and elasticity problems.

The next problematic case is related specifically to the transformation of variables used for subdomain edges. An example case is shown in Figure 5.1 and originated from a decomposition of a cube domain into 64 subdomains obtained using the graph partitioner Metis [13]. The subdomain edge  $E$  common to subdomains 3, 31, and 32 is shown as a solid line, while a finite element edge common to only subdomains 3 and 5 is shown as a dashed line. Notice that one of the endpoints of this edge is also an internal node of  $E$ . Recall that a transformation of variables is made for the edge degrees of freedom (dofs) of  $E$  so that two of them are explicitly primal. An unanticipated consequence of this transformation is that the subject finite element edge is now coupled to all the internal nodal dofs for  $E$  even though it is only *connected* to one of the nodes of  $E$ . This later led to a singularity in the partially assembled matrix  $\tilde{S}_F$ . The solution here is to simply split the original edge into two at the node common to  $E$  and the *problematic* finite element edge. We note for this example there were originally 660 subdomain edges. Of these, 7 had two disconnected components while only 2 had this problematic case.

An example of the third problematic case is shown in Figure 5.2 and was observed for a decomposition of a cube into 514 subdomains (512 subdomains requested, but

FIG. 5.1. *Second problematic subdomain edge case.*FIG. 5.2. *Third problematic subdomain edge case.*

two had disconnected components). Notice that the subdomain edge has three rather than two endpoints. Here the solution is to simply split the subdomain edge at any node incident to more than two finite element edges. For the example shown, this results in the original edge being split into three. We note for this example there were originally 7090 subdomain edges. Of these, only 1 had this problematic case.

**6. Numerical Examples.** Numerical examples are presented in this section to confirm the theory and to demonstrate the importance of deluxe scaling in certain cases. The number of preconditioned conjugate gradient iterations and associated condition number estimates to achieve a relative residual tolerance of  $10^{-8}$  for the solution of  $\widehat{S}_\Gamma x = b$  are denoted by *iter* and *cond* in the tables. The subdomains are discretized using the lowest order hexahedral edge elements, and random vectors  $b$  are used for all the examples. Unless stated otherwise deluxe scaling is used. We note that, we easily could have developed our theory for hexahedral elements in the same way as for tetrahedral edge elements.

TABLE 6.1

Results for unit cube decomposed into smaller cubical subdomains with  $H/h = 4$ . The material properties are constant with  $\alpha_i = \alpha$  and  $\beta_i = 1$ .

$N_d$	$\alpha = 10^{-4}$		$\alpha = 10^{-2}$		$\alpha = 1$		$\alpha = 10^2$		$\alpha = 10^4$	
	iter	cond	iter	cond	iter	cond	iter	cond	iter	cond
2	9	2.49	8	1.59	10	1.99	10	2.03	10	2.03
4	12	2.36	10	1.79	14	2.63	15	2.70	16	2.70
6	11	2.12	12	2.07	15	2.81	16	2.88	17	2.88
8	11	2.02	13	2.25	15	2.87	16	2.95	17	2.95
10	11	1.97	13	2.35	16	2.91	17	2.98	18	2.98
12	11	1.92	14	2.44	16	2.93	17	2.99	18	2.99

TABLE 6.2

Results for unit cube decomposed into 27 smaller cubical subdomains. The material properties are constant with  $\alpha_i = \alpha$  and  $\beta_i = 1$ .

$H/h$	$\alpha = 10^{-7}$		$\alpha = 10^{-2}$		$\alpha = 1$		$\alpha = 10^2$		$\alpha = 10^4$	
	iter	cond	iter	cond	iter	cond	iter	cond	iter	cond
4	12	2.74	9	1.63	13	2.41	13	2.47	14	2.47
6	15	4.51	12	2.15	14	2.93	15	3.01	16	3.01
8	19	6.89	14	2.70	16	3.34	17	3.44	18	3.44
10	22	9.98	15	3.22	17	3.69	18	3.79	19	3.79
12	24	13.8	16	3.69	17	3.98	19	4.09	20	4.10
14	28	18.3	17	4.13	18	4.24	19	4.36	21	4.36
16	30	23.5	18	4.55	19	4.47	20	4.60	22	4.60

The first example is for a unit cube decomposed into smaller cubical subdomains. The number of elements in each subdomain in each of the three coordinate directions is denoted by  $H/h$ . Similarly,  $N_d$  denotes the number of subdomains in each direction. The results in Table 6.1 confirm that condition numbers are bounded independently of the number of subdomains.

The next example fixes  $N_d = 3$  (27 subdomains) and varies  $H/h$  for constant material properties. Condition numbers from Table 6.2 for  $\alpha = 10^{-7}$  and  $\alpha = 10^4$ ,  $\beta = 1$ , are plotted versus  $H/h$  in Figure 6.1. Notice the fundamentally different dependence of condition number on  $H/h$  for very small and very large values of  $\alpha$ . In the case of very small  $\alpha$  (i.e. large  $\eta$ ), there appears to be at least a quadratic dependence of condition number on  $H/h$ . In contrast, for very large  $\alpha$  (small  $\eta$ ), condition numbers appear to be bounded by a multiple of  $(1 + \log(H/h))^2$ . Both of these observations are consistent with the theory.

REMARK 3. *In order to address the rapid growth in the condition numbers with respect to  $H/h$  for large values of  $\eta$ , we investigated the use of alternative transformations of variables for unknowns on subdomain edges. We found numerically for constant material properties that it is possible to get a uniform bound in  $H/h$  for  $\eta \gg 1$  while retaining the log-squared bound for  $\eta \ll 1$ . Nevertheless, rapid growth of the condition numbers was still observed for some intermediate values of  $\eta$ .*

The next example is used to confirm the theory for a checkerboard arrangement of material properties and to also demonstrate the importance of deluxe scaling in certain cases. As in the previous example, we consider a unit cube with  $N_d = 3$ , but now there are two sets of material properties. Red subdomains have  $(\alpha_i = 10^4, \beta_i = 10^{-2})$  while black subdomains have  $(\alpha_i = 10^2, \beta_i = 1)$ . We note that red subdomains share faces with black subdomains while red subdomains only share vertices with each other (the same holds for black subdomains). Results are shown in Table 6.3 for scaling based on matrix diagonal entries (stiffness scaling), the inverse of the number of subdomains

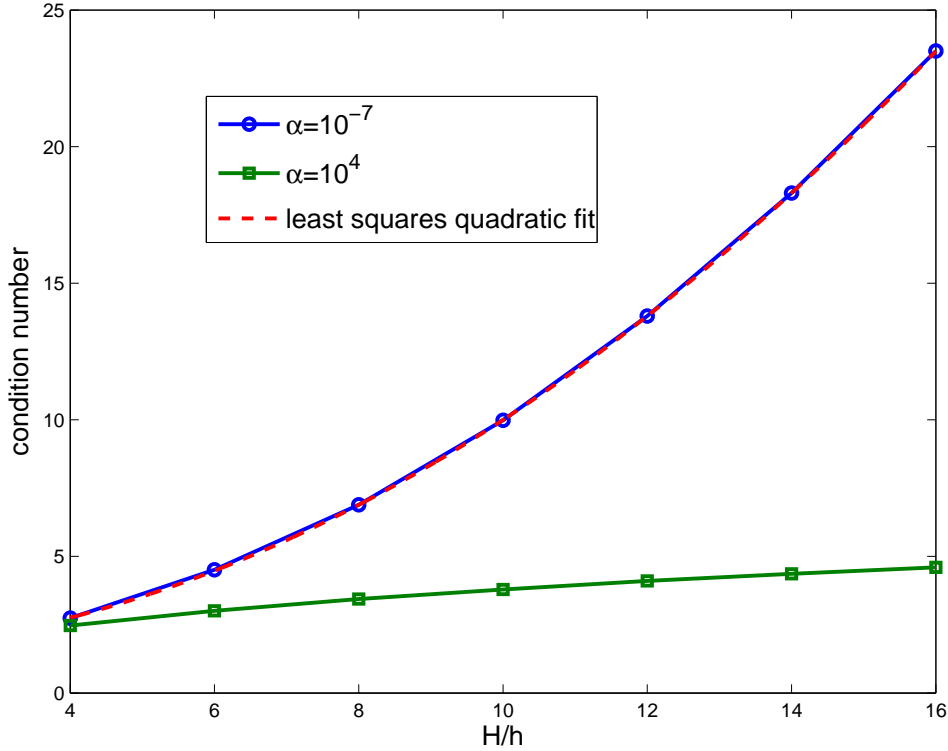


FIG. 6.1. Condition number estimates and least squares quadratic fit for  $\alpha = 10^{-7}$  and  $\alpha = 10^4$ .

TABLE 6.3

Results for unit cube decomposed into 27 smaller smaller cubical subdomains with a checkerboard arrangement of material properties.

$H/h$	stiffness scaling		cardinality scaling		deluxe scaling		e-deluxe scaling	
	iter	cond	iter	cond	iter	cond	iter	cond
4	50	272	80	156	6	1.06	6	1.06
6	67	342	100	207	7	1.20	7	1.20
8	78	398	117	247	8	1.33	8	1.33
10	87	445	128	281	9	1.45	9	1.45
12	95	486	140	310	10	1.55	10	1.55
14	102	522	151	336	10	1.63	10	1.63
16	109	554	160	360	11	1.71	11	1.71

sharing an edge (cardinality scaling), deluxe scaling, and an economic version of deluxe scaling (e-deluxe scaling). With reference to Subsection 2.2, the economic version of deluxe scaling is obtained by only considering the interior edges of  $\Omega_i$  directly adjacent to the edges of  $F$  or  $E$  when determining the Schur complements  $S_F^{(i)}$  and  $S_E^{(i)}$ , respectively. We note this economic alternative can result in significant computational savings. Notice that condition numbers and iterations for deluxe scaling and its economic version are indistinguishable and much smaller than those for the other two standard scaling options. Further, the observed growth in condition number with  $H/h$  is consistent with the theoretical log-squared bound.

The final example is identical to the first, but now the subdomains are obtained

TABLE 6.4

Counterpart of Table 6.1 for subdomains obtained using a graph partitioner. Again, the material properties are constant with  $\alpha_i = \alpha$  and  $\beta_i = 1$ .

		deluxe scaling									
		$\alpha = 10^{-4}$		$\alpha = 10^{-2}$		$\alpha = 1$		$\alpha = 10^2$		$\alpha = 10^4$	
$N$	iter	cond	iter	cond	iter	cond	iter	cond	iter	cond	
8	13	2.94	10	1.83	13	2.60	13	2.65	14	2.66	
64	15	2.92	12	2.07	16	3.43	17	3.52	18	3.52	
217	16	3.30	14	2.74	19	3.87	20	3.91	21	3.92	
514	15	2.83	15	2.94	19	4.01	20	4.04	21	4.04	
		e-deluxe scaling									
8	13	2.94	10	1.83	13	2.70	13	2.76	14	2.76	
64	15	2.93	12	2.08	16	3.50	17	3.60	18	3.60	
217	16	3.30	14	2.74	19	3.94	20	3.98	21	3.98	
514	15	2.83	15	2.89	19	3.93	20	3.96	21	3.96	

using the graph partitioner Metis rather than using all cubical subdomains. For example, the counterpart of  $N_d = 4$  in Table 6.1 appears in the rows for  $N = 4^3 = 64$  in Table 6.4. Comparison of these two tables indicates that good performance of the algorithm is also possible for mesh decompositions obtained from graph partitioners. Notice also the comparable numbers of iterations and condition number estimates for the two deluxe scaling variants.

## REFERENCES

- [1] Susanne C. Brenner and Ridgway Scott. *The Mathematical Theory of Finite Element Methods*. Springer-Verlag, Berlin, Heidelberg, New York, 2008. Third edition.
- [2] Susanne C. Brenner and Li-Yeng Sung. BDDC and FETI-DP without matrices or vectors. *Comput. Methods Appl. Mech. Engrg.*, 196(8):1429–1435, 2007.
- [3] Lourenço Beirão da Veiga, Luca F. Pavarino, Simone Scacchi, Olof B. Widlund, and Stefano Zampini. Isogeometric BDDC preconditioners with deluxe scaling. Technical Report TR2013-955, Courant Institute, New York University, April 2013. To appear in SIAM J. Sci. Comput.
- [4] Clark R. Dohrmann and Olof B. Widlund. Some recent tools and a BDDC algorithm for 3D problems in  $H(\text{curl})$ . In Randolph Bank, Michael Holst, Olof Widlund, and Jinchao Xu, editors, *Domain Decomposition Methods in Science and Engineering XX*, number 91 in Lecture Notes in Computational Science and Engineering, pages 15–26, Heidelberg–Berlin, 2013. Springer. Proceedings of the Twentieth International Conference on Domain Decomposition Methods held at the University of California at San Diego, CA, February 9–13, 2011.
- [5] Maksymilian Dryja, Barry F. Smith, and Olof B. Widlund. Schwarz analysis of iterative substructuring algorithms for elliptic problems in three dimensions. *SIAM J. Numer. Anal.*, 31(6):1662–1694, 1994.
- [6] Ralf Hiptmair and Andrea Toselli. Overlapping and multilevel Schwarz methods for vector valued elliptic problems in three dimensions. In *Parallel solution of partial differential equations (Minneapolis, MN, 1997)*, volume 120 of *IMA Vol. Math. Appl.*, pages 181–208. Springer, New York, 2000.
- [7] Ralf Hiptmair, Gisela Widmer, and Jun Zou. Auxiliary space preconditioning in  $H_0(\text{curl}; \Omega)$ . *Numer. Math.*, 103(3):435–459, 2006.
- [8] Ralf Hiptmair and Jinchao Xu. Nodal auxiliary space preconditioning in  $H(\text{curl})$  and  $H(\text{div})$  spaces. *SIAM J. Numer. Anal.*, 45(6):2483–2509 (electronic), 2007.
- [9] Qiya Hu, Shi Shu, and Jun Zou. A discrete weighted Helmholtz decomposition and its applications. *Numer. Math.*, 125(1):153–189, 2013.
- [10] Qiya Hu, Shi Shu, and Jun Zou. A substructuring preconditioner of three-dimensional Maxwell’s equations. In Randolph Bank, Michael Holst, Olof Widlund, and Jinchao Xu, editors, *Domain Decomposition Methods in Science and Engineering XX*, number 91 in Lecture Notes in Computational Science and Engineering, pages 73–84, Heidelberg–Berlin, 2013. Springer. Proceedings of the Twentieth International Conference on Domain Decomposition

- Methods held at the University of California at San Diego, CA, February 9–13, 2011.
- [11] Qiya Hu and Jun Zou. A nonoverlapping domain decomposition method for Maxwell’s equations in three dimensions. *SIAM J. Numer. Anal.*, 41(5):1682–1708, 2003.
  - [12] Qiya Hu and Jun Zou. Substructuring preconditioners for saddle-point problems arising from Maxwell’s equations in three dimensions. *Math. Comp.*, 73(245):35–61 (electronic), 2004.
  - [13] George Karypis. *METIS, A Software Package for Partitioning Unstructured Graphs, Partitioning Meshes, and Computing Fill-Reducing Orderings of Sparse Matrices, Version 5.1.0*. University of Minnesota, Department of Computer Science and Engineering, Minneapolis, MN, 2013.
  - [14] Axel Klawonn, Olof B. Widlund, and Maksymilian Dryja. Dual-primal FETI methods for three-dimensional elliptic problems with heterogeneous coefficients. *SIAM J. Numer. Anal.*, 40(1):159–179, April 2002.
  - [15] Tzanio V. Kolev and Panayot S. Vassilevski. Parallel auxiliary space AMG for  $H(\text{curl})$  problems. *J. Comput. Math.*, 27(5):604–623, 2009.
  - [16] Jong Ho Lee. A balancing domain decomposition by constraints deluxe method for numerically thin Reissner-Mindlin plates approximated with Falk-Xu finite elements. Technical Report TR2013-958, Courant Institute, New York University, August 2013.
  - [17] Jing Li and Olof B. Widlund. FETI-DP, BDDC, and Block Cholesky Methods. *Internat. J. Numer. Methods Engrg.*, 66(2):250–271, 2006.
  - [18] Jan Mandel, Clark R. Dohrmann, and Radek Tezaur. An algebraic theory for primal and dual substructuring methods by constraints. *Appl. Numer. Math.*, 54:167–193, 2005.
  - [19] Jean-Claude Nédélec. Mixed finite elements in  $R^3$ . *Numer. Math.*, 35:315–341, 1980.
  - [20] Duk-Soon Oh, Olof B. Widlund, and Clark R. Dohrmann. A BDDC algorithm for Raviart-Thomas vector fields. Technical Report TR2013-951, Courant Institute, New York University, February 2013.
  - [21] Andrea Toselli. Overlapping Schwarz methods for Maxwell’s equations in three dimensions. *Numer. Math.*, 86:733–752, 2000.
  - [22] Andrea Toselli. Dual-primal FETI algorithms for edge finite-element approximations in 3D. *IMA J. Numer. Anal.*, 26:96–130, 2006.
  - [23] Andrea Toselli and Olof Widlund. *Domain Decomposition Methods - Algorithms and Theory*, volume 34 of *Springer Series in Computational Mathematics*. Springer-Verlag, Berlin Heidelberg New York, 2005.
  - [24] Barbara I. Wohlmuth, Andrea Toselli, and Olof B. Widlund. An iterative substructuring method for Raviart-Thomas vector fields in three dimensions. *SIAM J. Numer. Anal.*, 37(5):1657–1676, 2000.